Fouling Characterization and Treatment of Water Reuse Concentrate with Membrane Distillation: Do Organics Really Matter

In preparation for

Desalination

November 9, 2022

Luke Presson[a,b], Varinia Felix[a,b], Mukta Hardikar[a,b], Andrea Achilli[a,b], Kerri Hickenbottom[a,b*]

[a]Department of Chemical and Environmental Engineering, University of Arizona, Tucson, Arizona 85721, United States

[b]Water and Energy Sustainable Technology (WEST) Center, University of Arizona, Tucson, Arizona 85745, United States

*Corresponding Author: Kerri Hickenbottom, email: klh15@arizona.edu

Keywords:

Membrane Distillation, Water Reuse, Zero Liquid Discharge, Membrane Fouling, High Performance Liquid Chromatography

Highlights:

- Fouling and scaling by concentrated reclaimed water were investigated in MD
- A novel method to assess the hydrophobicity of natural organic matter is proposed
- Scaling was the main cause of water flux decline from concentrated reclaimed water
- The natural organic matter in treated wastewater was hydrophilic
- Calcium removal was an effective pretreatment for maintaining a high water flux

Abstract:

Membrane distillation (MD) for the treatment of concentrated brines has been limited in part by membrane fouling and subsequent flux decline and membrane wetting. This study provides new insight into the identification of fouling and scaling mechanisms and pretreatment strategies for mitigating flux decline with MD treatment of water reuse reverse osmosis concentrate (ROC). Bench-scale direct contact MD experiments were performed with untreated and pretreated ROC. Biological activated carbon (BAC), chemical water softening, or ion exchange coupled with a fluidized bed crystallization reactor (FBCR) were selected as pretreatment strategies to isolate the effects of organic fouling and calcium scaling. Organic and inorganic compounds were analyzed by High-Performance Liquid Chromatography (HPLC) and inductively coupled plasma mass spectrometry (ICP-MS). Calcium ions were found to be the major contributor to flux decline despite the high organic content in the ROC. Minimal organic fouling is likely because the organic matter in the ROC is hydrophilic, limiting hydrophobic-hydrophobic interactions between the organics and the membrane. Furthermore, the water flux declined by 63 percent after removing organic compounds by BAC pretreatment, with 60 percent of the calcium mass precipitating from the solution. Whereas, the water flux remained constant after removing multivalent ions with fluidized bed crystallization. Cleaning the membrane by acid washing and temperature reversal recovered 73 percent and 12 percent of the water flux, respectively. The analyses outlined in this study can assist in selecting appropriate fouling and scaling mitigation strategies for water reuse ROC and a wide range of feed solutions used in MD applications.

1. Introduction

Implementation of reverse osmosis (RO) for water reuse has been limited by the lack of environmentally responsible and economically viable disposal methods for the RO concentrate (ROC) [1]. Typical water recovery from the industry standard treatment train ranges from 60 to 80 percent [2, 3]—thus generating a relatively large waste stream containing high concentrations of organic and inorganic compounds, including pharmaceuticals and personal care products and sparingly soluble salts that need to be appropriately managed. Minimizing the volume of brine is termed zero liquid discharge (ZLD) and is of particular importance for water-stressed inland regions where options for brine disposal are limited.

MD has been demonstrated as a promising technology to minimize brine volume while purifying contaminated waters using low-grade thermal energy [4-7]. In MD, a heated concentrate stream and a cooler condensing stream flow across either side of a microporous hydrophobic membrane. The temperature gradient between the feed stream and the condensing side of the membrane induces a partial vapor pressure gradient that drives the desalination process: water evaporates at the feed-membrane interface, diffuses through the membrane pores, and condenses as high-quality distillate. Because water mass transport occurs in the vapor phase, MD is theoretically capable of rejecting 100% of non-volatiles. When using concentrated brines in MD, the high salinity lowers the driving force, but the physical stress on the membrane remains low—an advantage over pressure-based membrane processes like RO. High rejection and resilience to feed solutions with high osmotic pressure make MD well suited for treating concentrated brines, including industrial wastewaters [8, 9], produced waters [10-12], and RO brines [13-15].

Although the water recovery of a combined RO-MD system can be above 96% [13, 16], the water flux and high rejection in MD are compromised by membrane fouling and scaling: the adhesion of organic (fouling) and inorganic (scaling) compounds to the membrane. Fouling and scaling are exacerbated by concentration polarization, as evaporation at the membrane surface results in higher solute concentrations at the membrane interface than in the bulk solution [17]. Fouling and scaling are also heavily influenced by the membrane surface characteristics. Hydrophobic membranes can slow or prevent fouling and scaling by forming a Cassie-Baxter state [18]. In MD, the Cassie-Baxter state develops when a membrane with high porosity and low surface energy interacts with water. The rough, hydrophobic surface forms small air pockets between the membrane and liquid, decreasing the contact area between the feed solution and membrane [19-21]. The Cassie-Baxter state is contrasted with the Wenzel state [22], in which the porous surface is less hydrophobic, and the solution fully contacts the surface of the membrane. Researchers have taken advantage of the Cassie-Baxter state to design omniphobic membranes that repel contaminants with high surface tension and waters with low surface tension [23, 24].

Fouling and scaling can decrease membrane hydrophobicity and deform pores leading to membrane wetting—a critical flaw in MD when the feed solution flows through the pore in the liquid phase—compromising membrane rejection. Wastewater and water reuse brine has been shown to cause flux decline and membrane wetting in MD [15, 25-28]. Mixed streams like municipal wastewater and water reuse concentrate have many different foulants and scalants over a wide range of concentrations. The variability and complexity of these feed streams make isolating fouling and scaling mechanisms and mitigation strategies difficult.

A proposed mechanism for membrane fouling is adhesion through hydrophobic-hydrophobic interactions [29]. Hydrophobic particles have a stronger attraction to the hydrophobic membrane than their hydrophilic counterparts [30], but identifying the characteristics of organic compounds in real waters is difficult. There is an established method for characterizing the molecular size of natural organic matter [31], but current methods to characterize the hydrophobicity of organics are less reliable. One method—specific UV absorbance (SUVA)—is often used to estimate the aromaticity of dissolved organic matter and is calculated as the UV absorbance at 254nm divided by the organic concentration [32]. Unfortunately, using the SUVA method for assessing the hydrophobicity of some natural organic matter can be misleading. For example, humic substances have high SUVA values but are hydrophilic in neutral pH ranges [33, 34]. Fluorescence excitation-emission (EEM) spectroscopy is another method that can be performed rapidly and may give statistically significant information about the hydrophobicity of DOM [35]. However, this information relies upon correlational and specific analysis focusing on natural organic matter, which may not be the only organic matter in MD applications. Therefore, understanding fouling mechanisms and selecting mitigation strategies in MD applications needs a more robust and direct measurement of feed solution hydrophobicity.

Scaling by inorganic salts is caused by precipitation on the membrane surface (heterogeneous nucleation) or precipitation in the bulk solution (homogenous nucleation) and subsequent settling onto the membrane [36]. Two of the ions commonly responsible for scaling in MD are calcium and silicon. Gypsum crystals can block and deform pores leading to rapid water flux decline and membrane wetting [37]. Calcium ions can also precipitate as calcite or in complexation with organic compounds and cause severe flux decline [38, 39]. Silica scaling occurs more slowly than calcium salts like gypsum because silicic acid polymerizes more slowly than gypsum

crystallizes [37]. Silica scaling is also most detrimental at neutral pH ranges [40]. Even NaCl solutions can cause flux decline when present at supersaturated concentrations [41, 42]. Precipitation of some calcium salts like gypsum is also affected by high temperatures because they are less soluble at high temperatures [43]. Some commonly proposed scaling mitigation methods include bulk filtration [44] and antiscalant addition[45]. The use of a simple cartridge filter has been shown to aid in flux decline by removing precipitated salts before they reach the membrane [46]. Antiscalants can hinder the precipitation and crystal formation of sparingly soluble salts, but their use is highly dependent on MD operating conditions [47].

The objective of this research is to identify fouling and scaling mechanisms and mitigation strategies when using water reuse ROC as the feed solution for MD treatment. ROC from the Agua Nueva Water Reclamation Facility (Tucson, AZ) was used to assess flux decline in bench scale MD experiments. Pretreatments were applied to isolate the effects of fouling and scaling and membrane cleaning methods were evaluated for recovering water flux. The mass precipitated of scalants including calcium, silicon, and magnesium were calculated and a membrane autopsy was performed to identify key scalants. A novel analytical method was developed to characterize the hydrophobicity of organic compounds present in the feed solution. The developed method can be used to assess the likelihood of hydrophobic-hydrophobic interactions between the MD membrane and potential feed solutions. The methods outlined are designed to be generalizable to a wide range of MD applications.

2. Materials and Methods

2.1 Membrane and MD Bench-Scale System

Direct contact MD (DCMD) experiments were performed with a polytetrafluoroethylene (PTFE) membrane with a polypropylene (PP) support layer (Clarcor QL822, Parker Hannifin, Lee's Summit, MO). The membrane water entry pressure, nominal pore size, porosity, and thickness was 2.5 bar, 0.45µm, 70 to 85 percent, and 127-203µm, respectively. The membrane was placed in an acrylic cell with extruded mesh spacers on either side of the membrane and had an active membrane surface area of 13.8 cm^2.

A flow schematic of the DCMD system is illustrated in Figure 1. Two gear pumps (Cole Parmer, Vernon Hills, IL) circulated the feed and permeate solutions through the heat exchangers (Alfa heating, Derwood, MD) and the MD module at 1.6 L/min. The temperatures of the feed and permeate streams were held constant at 70°C and 30°C, respectively, with an in-line heater (Omega, Norwalk, CT) and recirculating chiller (Thermo Fisher Scientific, Waltham, MA). Water temperature, turbidity, and conductivity were monitored with K-type temperature sensors (Cole Parmer), an in-line TU5400 turbidimeter (Hach, Loveland, CO), and a conductivity meter (Oakton Instruments, Vernon Hills, IL), respectively. The water flux was calculated by utilizing an overflow system and analytical balance (Ohaus, Parsippany, NJ) that recorded the mass of water permeated across the membrane over time. In each experiment, samples of the feed solution were taken at regular intervals. The mass precipitated at each interval was calculated using the concentration of the ions in the feed sample and the volume remaining in the feed stream.

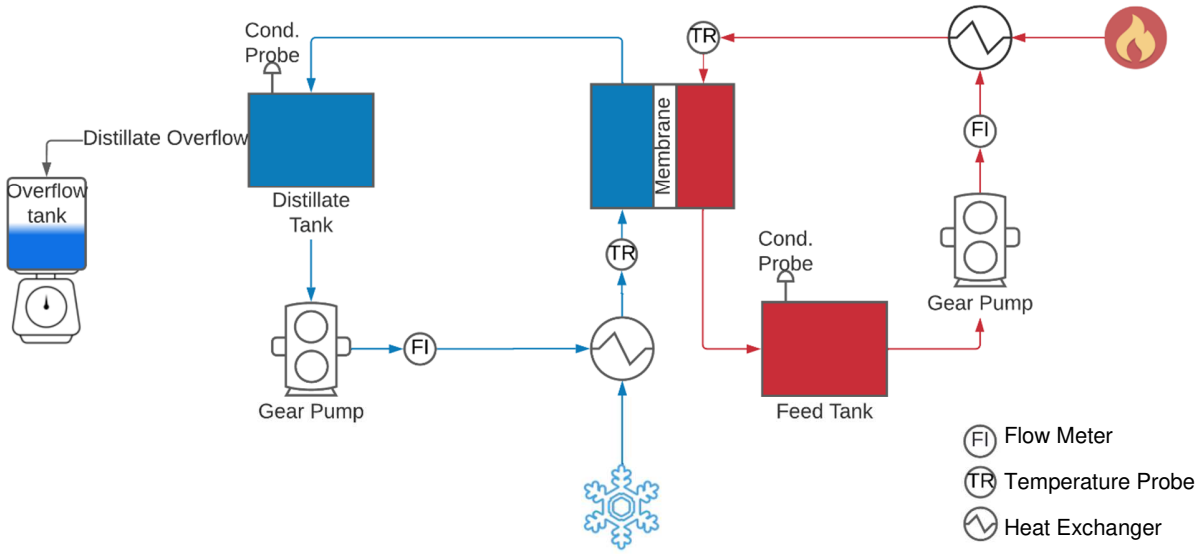

Figure 1. Schematic of the bench-scale MD system. The blue section on the left represents the distillate side of the membrane, and the red section on the right represents the feed stream. Batch cycles were performed with a starting feed solution volume of 5L each of fresh ROC and circulated at 1.6 L/min at 70°C and 30°C for the feed and distillate, respectively.

The starting batch volume in all experiments was 5L of feed solution (ROC or pretreated ROC) and was recirculated until 60 to 70 percent recovery. All experiments were performed with three batch cycles using fresh ROC and the same membrane, except for one experiment performed with reconstituted ROC. In the reconstituted ROC experiment, the first batch cycle was concentrated to 70 percent recovery. After the first batch cycle, the feed solution was reconstituted to 5 L with deionized (DI) water and reconcentrated. DI water was used for reconstitution in batch cycles 2 and 3 to bring the feed solution to the same starting volume as other experiments (5 L) without adding solutes to the system. Three batch cycles were performed with reconstituted feed.

2.2 Brine collection and treatment

Water reuse ROC was collected from a pilot-scale ultrafiltration-RO system treating secondary effluent from the Agua Nueva Water Reclamation Facility. The ROC was used as the feed solution for all DCMD experiments. Additional experiments were performed with batches of pretreated ROC by either biological activated carbon (BAC) filtration, chemical water softening, or ion exchange coupled with a fluidized bed crystallization reactor (FBCR). The BAF column residence time for 95 percent removal of TOC was 45 minutes at 65 rpm; additional information on the columns and acclimation procedure can be found in the supporting information. The chemical water softening was performed by adjusting the room temperature ROC to pH 11 (pH meter, Oakton Instruments, Vernon Hills, IL) with a 3 M NaOH (Sigma Aldrich, Burlington, MA) solution. The pH adjusted ROC solution was allowed to settle and was then decanted into a secondary container. The decanted ROC was neutralized to pH 8 by the addition of concentrated HCl (Fischer Chemical, Waltham, MA). Details on the ion exchange and FBCR pretreatment can

be found in prior work [48], [49]. The saturation of calcite and silica at 70 °C for untreated and treated ROC was calculated with OLI software (OLI Studio Inc., Cedar Knolls, NJ). The compositions of treated and untreated feed solutions are summarized in Table 1. The untreated ROC batch was collected separately from the other solutions and therefore had slightly different characteristics

Table 1: Concentrations of dissolved compounds and water quality parameters in untreated and pretreated ROC with chemical softening, BAC, and FBCR-ion exchange (IX).

Pretreatment	Na^+ (mg/L)	Mg^{2+} (mg/L)	Ca^{2+} (mg/L)	Si (mg/L)	TOC (mg/L)	pH	Conductivity (mS/cm)
Untreated	293	59	431	94	26	8	3.83
Softened	389	93	60	59	21	8	4.61
BAC	275	105	435	50	1	8	4.85
FBCR-IX	349	0	2.4	33	24	8	2.65

2.3 Membrane Cleaning

Cleaning experiments were performed on the membrane fouled with untreated ROC. The cleaning methods include acid washing, base washing, and temperature reversal. Each of these cleaning methods was performed sequentially on the same membrane using the same operating conditions as the batch ROC experiments. After each cleaning experiment, the water flux of the cleaned membrane was determined by performing DCMD experiments with DI as the feed and permeate solution using the same conditions as the batch ROC experiments.

The fouled membrane was cleaned via acid or base washing by circulating either 2% HNO_3 (pH 0.52) or 0.1 M NaOH (pH 13) at 1.6 L/min for one hour on the feed side of the membrane cell. The temperature reversal cleaning procedure was performed by circulating DI water at 1.6 L/min on either side of the membrane for one hour. However, the feed and permeate stream temperatures were maintained at 30°C and 70°C, respectively, effectively reversing the driving force or direction of water vapor across the membrane (i.e., distillate side to feed side of the membrane) [50].

2.4 Analytical Methods

2.4.1 Ion Analysis

Cation concentrations were measured using an Agilent 7800x Series Inductively Coupled Plasma Mass Spectrometer (ICP-MS) (Agilent, Palo Alto, CA) in helium collision gas mode. Samples

were centrifuged at 3000 RPM for 15 minutes before aliquots were diluted with 2% HNO_3 (tracemetal grade, Fisher Chemical, Waltham, MA). The concentration values reported are the average of three measurements.

2.4.2 Organic Analysis

The total organic carbon (TOC) was measured using a Shimadzu TOC-L CSH Total Organic Carbon analyzer (Shimadzu Corp., Japan). TOC samples were acidified with 70 µL of HCl (Fischer Chemical, Waltham, MA).

A novel nontargeted reverse phase chromatography method was developed to assess the hydrophobicity of organic compounds using an Agilent 1260 II HPLC with an in-line diode array detector (Agilent 1260 DAD) set at 254 nm. The HPLC was equipped with an Agilent Poroshell 120 EC-C18 column and a mobile phase consisting of water and methanol at a flow rate of 0.3 mL/min. A gradient elution method was developed to adequately separate compounds based on their hydrophobicity and validated with standard compounds (Sigma Aldrich, Burlington, MA). The standards used and their computationally estimated $\log K_{ow}$ values[51]—a surrogate measurement for hydrophobicity—are summarized in Table 2.

Table 2: Hydrophobicity standards and their estimated $\log K_{ow}$ values.

Compound	Uracil	Caffeine	Acetophenone	Naphthalene
$\log K_{ow}$	-1.07	-0.07	1.58	3.30

2.4.3 Membrane Autopsy

Membranes were analyzed using an FEI Inspec-S scanning electron microscope (SEM) with energy dispersive x-ray spectroscopy (EDS, FEI Company, Hillsboro, OR). Membrane hydrophobicity was established by contact angle measurement using the sessile drop method, where DI water was the medium, with a Krüss DSA25E goniometer (Krüss Scientific, Hamburg, Germany). Membrane charge was assessed by determining the zeta potential with an Anton Paar SurPASS 3 analyzer (Anton Paar, Graz, Austria). Each autopsy method was performed with multiple measurements and values reported are the average of all measurements.

3. Results and Discussion

3.1 Water Flux Experiments with Untreated ROC

The water flux, change in water flux per time, and turbidity as a function of percent water recovery with untreated ROC are presented in Fig. 2. The water flux remains relatively constant throughout the first batch cycle. In the second batch cycle most of the water flux decline occurs in the first half of the experiment. In the third cycle, a large decline in water flux occurs before 30% recovery and is relatively constant from 30 to 50 percent recovery before beginning to decline at an increasing rate. The turbidity of the first batch cycle was monitored and reaches a maximum at five percent recovery and then precipitously declines to <5 NTU. The initial increase in turbidity is likely homogenous precipitation of calcium compounds (i.e., calcium

carbonate) in the bulk solution. OLI simulations confirm that the initial concentration of calcium carbonate in ROC is supersaturated at 70°C, thus calcium carbonate is likely to have precipitated

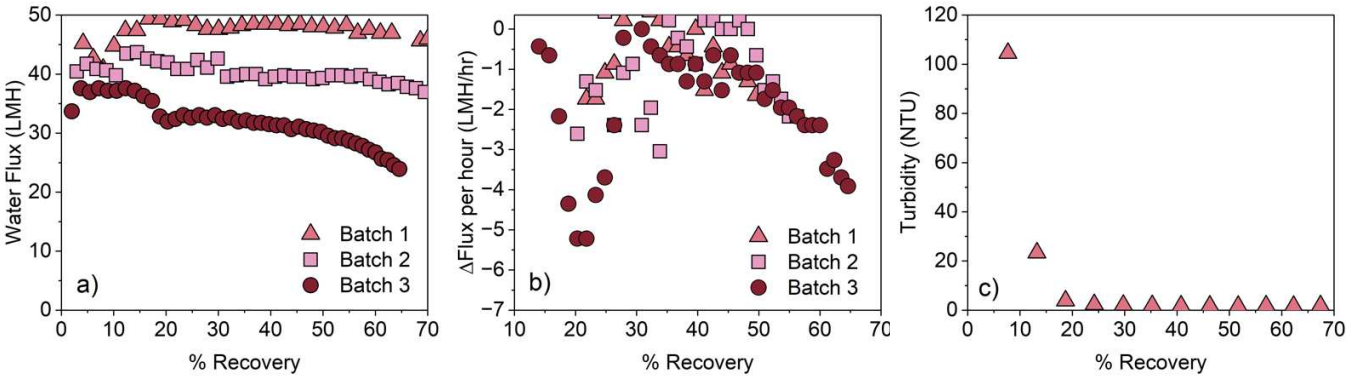

on the membrane. In each batch cycle the distillate conductivity remained constant and below 10 µS/cm (Fig. S1 in SI).

Figure 2. (a) Water flux, (b) the change in water flux per hour, and (c) the turbidity of the first batch cycle as a function of percent recovery for untreated ROC. Batch cycles were performed with a starting feed volume of 5L each of fresh ROC and circulated at 1.6 L/min at 70°C and 30°C for the feed and distillate, respectively. Distillate conductivity remained constant in each batch cycle.

The normalized water flux before and after cleaning the membrane is shown in Fig. 3. Cleaning the membrane with a 2% HNO_3 solution for one hour recovered 73 percent of the water flux. In contrast, cleaning the membrane with 0.1 M NaOH did not recover additional water flux. Whereas temperature reversal recovered an additional 12 percent of water flux. The acid solution was collected after cleaning and analyzed by ICP-MS. The concentration of calcium in the acid solution (220 mg/L) was 50 times higher than magnesium (4.4 mg/L), and silicon was not detected (<0.1 mg.L). Therefore, the large increase in recovered water flux by acid washing is likely from acid-induced dissolution of calcium carbonate ($\log K_{sp}$ = 8.48). The temperature reversal cleaning method displaces particulates adhered to the membrane and pores by reversing

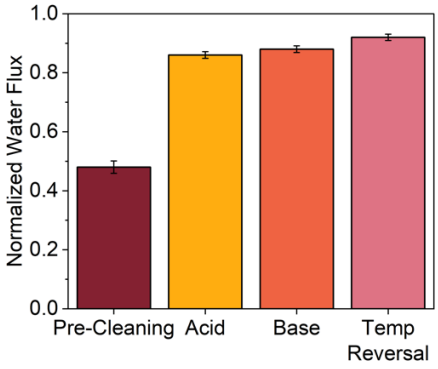

the passage of water vapor from the support to the active side of the membrane [42, 52].

Figure 3. The normalized water flux after sequential membrane cleanings for the fouled membrane from the MD experiments performed with untreated ROC. Cleaning experiments were performed sequentially on a membrane fouled with untreated ROC. Acid and base washing involved circulating 2 % HNO_3 and 0.1 M NaOH in the feed side of the membrane cell. Temperature reversal was performed by reversing the driving force and direction of water vapor transport. The feed and distillate streams were circulated at 1.6 L/min. For the acid and base cleaning, the feed and distillate streams were kept constant at 70°C and 30°C, respectively. Whereas for the temperature reversal cleaning, the distillate and feed streams were kept constant at 70°C and 30°C, respectively. After each cleaning procedure the water flux was determined by circulating DI water at the experimental conditions until the water flux was stable for several measurements.

Untreated ROC was again concentrated with a new membrane, but batch cycles 2 and 3 were performed with reconstituted ROC. After the first batch was concentrated to 70 percent recovery, DI water was added to return the feed solution volume to 5L without introducing more foulants or scalants to the system. Batch cycles 4 and 5 were performed with fresh ROC. The water flux as a function of percent recovery for the reconstituted ROC experiments is shown in Fig. 4a. The water flux remained relatively constant during the first three batch cycles performed with reconstituted ROC; however, the initial water flux declined and continued to decline throughout the experiment when fresh ROC is used as the feed solution in batches 4 and 5. The concentration of sodium, magnesium, silicon, and calcium at the beginning of the experiments and after the first three batch cycles with reconstituted ROC is shown in Fig. 4b. The concentration of sodium, magnesium, silicon, and calcium decline by 0.7, 20, 38, and 55 percent, respectively, after the first batch cycle (Table S1 in SI). In subsequent batch cycles 2 and 3 using the reconstituted ROC, the calcium concentration remains the same and only a small amount of magnesium and silicon precipitate. The small variation of cation concentration in reconstituted batches 2 and 3 is evidence that there was minimal precipitation and water flux decline when the reconstituted ROC was exposed to the membrane for a longer time period (Figure 4 b). Further membrane scaling was only observed when more scalants were added to the system (fresh ROC, batch cycles 4 and 5). Therefore, the initial water flux decline in subsequent batch cycles 4 and 5 are likely from membrane scaling. Based on these observations, pretreatment experiments were performed to isolate the organics and scalants from the ROC and further assess the mechanisms for membrane scaling.

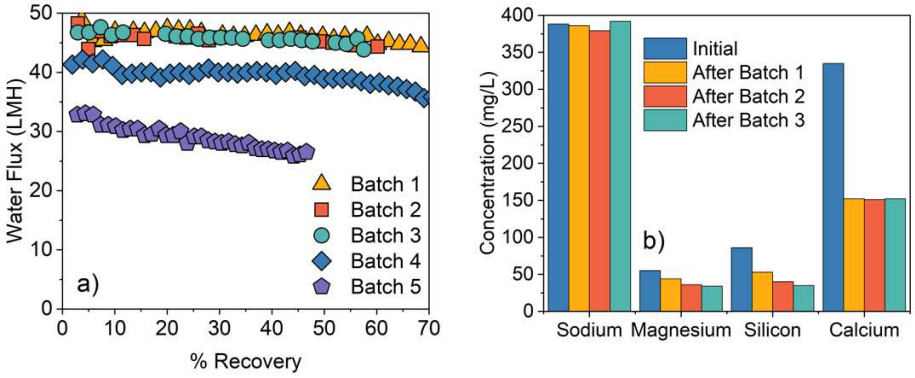

Figure 4. (a) The water flux as a function of percent recovery and (b) the concentration of various cations after the batch is reconstituted. After batch 1, the remaining volume is reconstituted with DI water and concentrated again as batch 2. The same procedure was performed for batch 2 and 3. Batches 4 and 5 represent cycles with fresh ROC. Batch cycles were performed with a starting feed volume of 5L each of ROC and circulated at 1.6 L/min at 70°C and 30°C for the feed and distillate, respectively. Distillate conductivity remained constant in each batch cycle.

3.2 Water Flux Experiments with Pretreated ROC

3.2.1 Comparison of Pretreatment Effectiveness

Concentration experiments with ion exchange-FBCR, softened, and BAC treated ROC were performed to compare pretreatment methods. The water flux and hourly change in water flux as a function of percent recovery for each feed solution are shown in Fig. 5. The BAC treated ROC had the highest concentration of calcium, but the lowest organic concentration. The water flux for the BAC treated ROC decreased rapidly in the first half of each batch cycle, leading to the largest water flux decline of the pretreatment experiments. The early water flux decline is likely from the immediate supersaturation of calcium carbonate upon reaching 70°C (Fig. S2 in SI). The softened ROC had a lower initial calcium concentration, but higher organic concentration than the BAC treated ROC. The water flux for the softened ROC remained constant through the first batch cycle and most of the second batch cycle. However, after 45 percent recovery in the second batch cycle the water flux declines by nearly 10 percent and continues to decline by another 20 percent in the third batch cycle. The water flux remained constant throughout each batch cycle when using the ion exchange-FBCR treated ROC despite having the highest concentration of organics. The constant water flux in the ion exchange-FBCR treated ROC is likely because it had the lowest calcium concentration. In each experiment the distillate conductivity remained constant and below 10 µS/cm (Fig. S1 in SI).

A previous study by Naidu et al. observed that calcium carbonate precipitates were not a large contributor to water flux decline and recommended granular activated carbon (GAC) pretreatment for its ability to remove micropollutants and maintain membrane hydrophobicity

[15]. Contrasting observations in this study are likely because of the difference in water chemistry of the feed solution. For example, the ROC utilized in our work had 488% higher calcium, likely leading to more calcium carbonate precipitation and water flux decline. Additionally, although BAC pretreatment was ineffective for mitigating water flux decline (Fig. 5 a,d), BAC may be useful for micropollutant removal. The lack of organic fouling may be further explained by the organic compounds in the feed solution having few hydrophobic-hydrophobic interactions with the membrane.

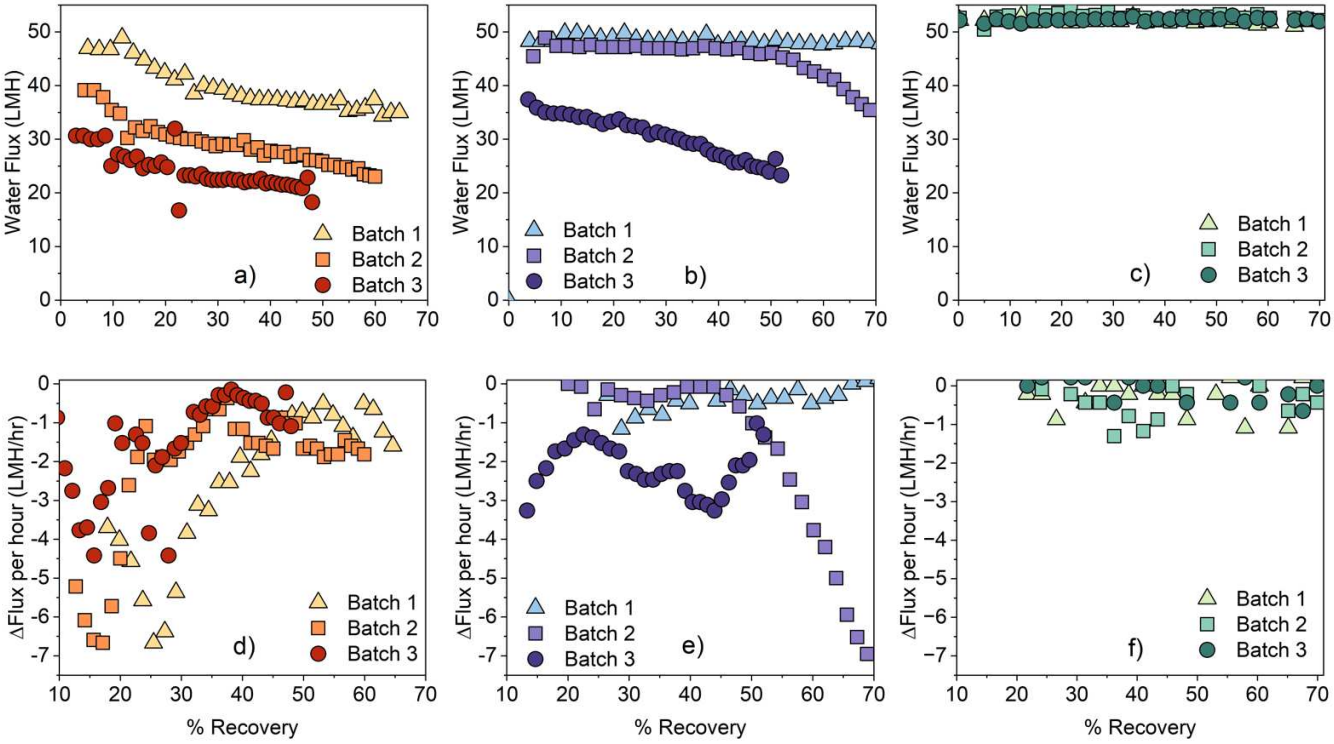

Figure 5. The water flux and the change in water flux per hour for (a,d) BAC treated, (b,e) softened, and (c,f) ion exchange-FBCR treated ROC as a function of percent recovery. Batch cycles were performed with a starting feed volume of 5L each of fresh ROC and circulated at 1.6 L/min at 70°C and 30°C for the feed and distillate, respectively. Distillate conductivity remained constant in all experiments.

3.3 Organic characterization

A reverse phase HPLC method was developed to assess the hydrophobicity of the organic matter present in the ROC. The most consequential parameters affecting the retention in reverse phase HPLC are the hydrophobicity and polarity of the stationary phase, mobile phase, and analyte [53, 54]. By keeping the stationary phase and mobile phase constant the proposed method aims to correlate the retention time of solutes to their hydrophobicity. The molecular size of solutes can have small effects on retention [55], but strong correlations between hydrophobicity and

retention have been documented for aromatic solutes [56]. First, standard compounds were tested to serve as a form of hydrophobicity calibration. The chromatogram of the standard compounds and their labeled peaks are illustrated in Fig. 6a. The standards elute in order of their hydrophobicity with the full range of standards eluting within 25 minutes.

The chromatogram of the untreated and BAC treated ROC is depicted in Fig. 6b. Peaks are only observed at low retention times corresponding to hydrophilic material. There is an increase in the baseline in both chromatograms at 10 minutes attributable to the effects of the gradient elution rather than organic compounds in the sample. Nearly all peaks of the ROC elute before five minutes and are therefore hydrophilic. Thus, the HPLC results confirm that organic fouling via hydrophobic-hydrophobic interactions is an unlikely mechanism for membrane fouling.

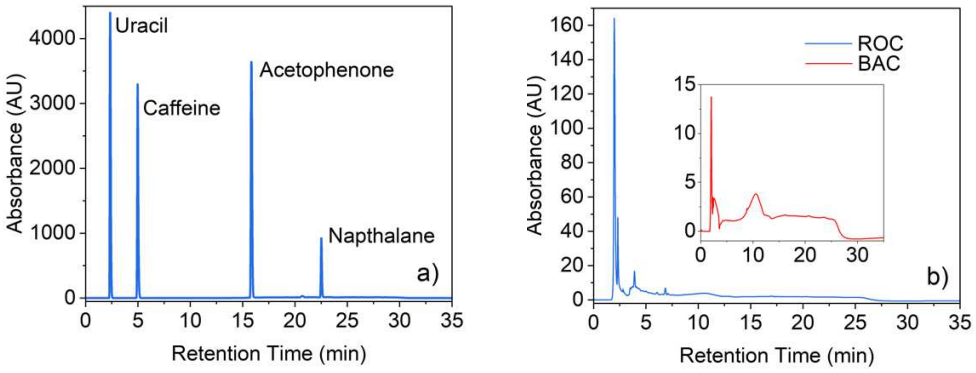

Figure 6. HPLC chromatogram of the hydrophobicity standards (a). From left to right the peaks correspond to uracil, caffeine, acetophenone, and naphthalene. HPLC chromatogram of untreated and BAC treated ROC (b).

3.4 Solute Mass Precipitated in Pretreatment Experiments

The cumulative mass of calcium, magnesium, and silicon as a function of distillate produced is shown in Fig. 7. In the BAC treated ROC, the mass of calcium precipitating is an order of magnitude larger than any other ion and is further evidence of the increased relative importance of calcium scaling. Interestingly, in the softened ROC more silicon precipitates. The high silicon precipitation is a surprising result because OLI simulations predict that silicon becomes supersaturated only after 55% recovery in the softened ROC. In previous studies, organic compounds have increased the water flux decline caused by silica scaling [57, 58]. Therefore, while there is little evidence of organic compounds fouling the membrane, their presence in the softened ROC may increase the flux decline caused primarily by complexation with other species like silicon. Precipitation of calcium, magnesium, and silicon was not observed when using the FBCR treated ROC because pre-treatment removed 99, 100 and 65 percent of these constituents, respectively. Note that the 1.6 L/min flow rate used in all experiments likely minimized concentration and temperature polarization compared to experiments performed with lower flow rates/velocities [59-61]. In systems that cannot reach the high flow velocities used in

this study, increased concentration and temperature polarization may affect the precipitation of ions, and lead to more scaling.

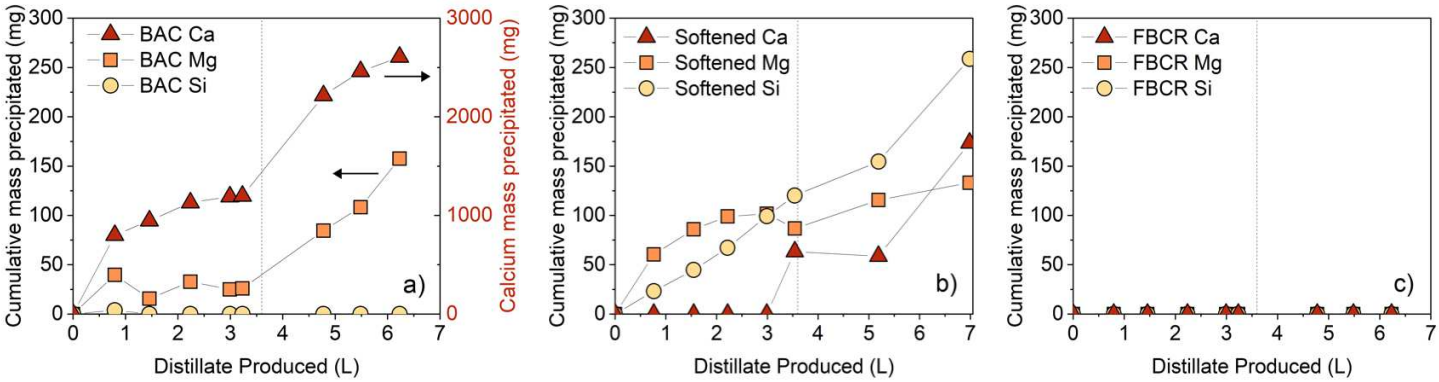

Figure 7: The mass of magnesium, silicon, and calcium precipitated as a function of distillate produced for (a) BAC treated ROC, (b) softened ROC, and FBCR treated ROC. The calcium mass precipitated in BAC treated ROC is displayed on a secondary axis because it is an order of magnitude larger than the other ions. Two successive batch cycles are shown separated by the dashed line at roughly 3.5 L of distillate produced.

3.5 Membrane Autopsy

EDS analysis was performed on the fouled membranes and the results are shown in Fig. 8. The calcium peak in the spectrum from the BAC treated ROC is larger than any other ion, which is consistent with the theory that calcium is the dominant scalant. Magnesium was detected in the spectrum from the BAC treated ROC, but is nearly indistinguishable from the baseline due to the size of the calcium peak. Different ion compositions were observed on the membrane fouled with softened ROC depending on where the measurement was taken. The main difference between locations was the relative responses of calcium, magnesium, and silicon. In one location the silicon and magnesium peaks were larger than the calcium peak, but in another location the calcium was much larger. Based on the EDS analysis and analysis of the cation mass precipitated during batch cycles (Fig. 7) it is likely that calcium, magnesium, and silicon were the primary contributors to membrane scaling in the experiment with softened ROC. Membrane scaling was localized as demonstrated in the SEM images (Fig. S3 in SI) in which the membranes scaled with softened ROC and FBCR treated ROC have crystals non-uniformly distributed on the surface. In contrast the membrane scaled with BAC treated ROC had scalants covering the entire membrane surface. Calcium and magnesium were not observed in the EDS analysis of the membrane fouled with FBCR treated ROC, and the largest peaks were from the PTFE membrane (fluorine) and the gold coating necessary for analysis. There is a small peak that could be trace amounts of silicon, but the result is consistent with the observation that the FBCR treated ROC did not foul or scale the membrane (Fig. 5c).

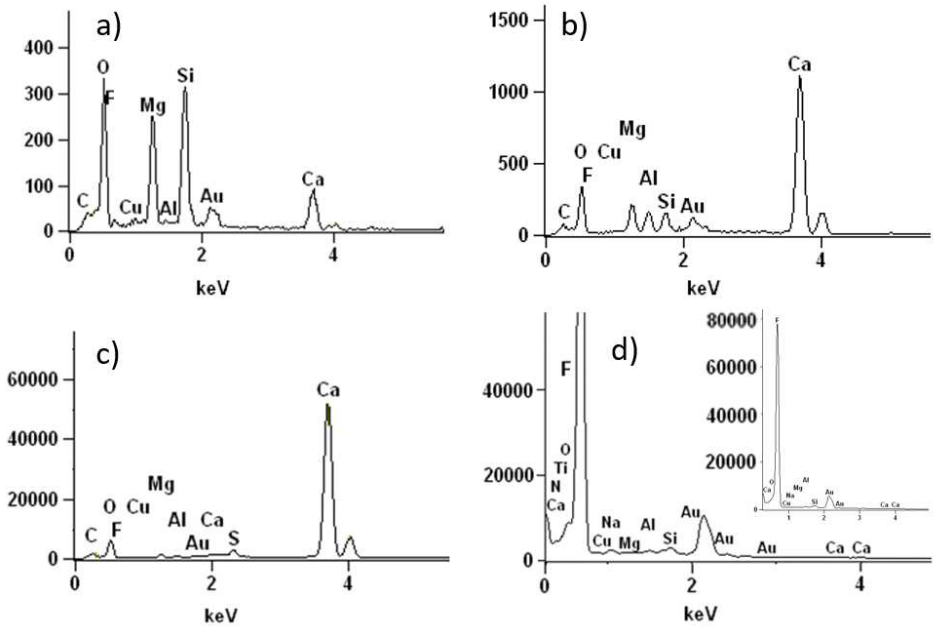

Figure 8. SEM-EDS analysis of fouled membranes. (a) and (b) membrane fouled with softened ROC with measurements taken at different locations on the membrane. (c) membrane fouled with BAC treated ROC. (d) Membrane fouled with FBCR treated ROC. The spectrum of the membrane fouled with FBCR treated ROC is formatted to show the baseline and includes an inlayed image to accurately depict the fluorine peak.

The contact angle and zeta potential of the virgin and fouled membranes are summarized in Table 3. The fouled membranes all had lower contact angles and were less negatively charged than the virgin membrane, but the changes were more severe for the membranes fouled with BAC treated and softened ROC. Despite the low contact angle, no wetting was observed as the conductivity of the distillate remained below 10µs/cm. Therefore, while the membrane contact angle decreased, the pores retained their hydrophobicity and prevented wetting [62]. Over longer-term studies scalants likely would infiltrate further into the pore, leading to pore flow and membrane wetting. The membrane fouled with BAC treated ROC was the least negatively charged because the larger amount of positively charged scalants present suppressed the charge of the membrane.

Table 3. The contact angle and zeta potential for virgin and fouled membranes.

Membrane	Contact Angle	Zeta Potential (mV)
Virgin	130°	-45.1
BAC Treated	<60°	-13.7
Softened	<60°	-19.7
FBCR Treated	102°	-31.2

The decrease in the contact angle of the fouled membranes is indicative of the transition from the Cassie-Baxter state to the Wenzel state and may explain the increasing rate of water flux decline observed in the softened ROC experiments. In the Cassie-Baxter state there is less membrane-liquid contact area for homogeneous precipitation to settle and adhere to the membrane compared to the Wenzel state. Heterogenous precipitation is decreased by similar logic as there is less contact between feed solution and membrane and therefore less availability for crystallization on the membrane surface. However, the small contact points between the membrane surface and solution slowly collect precipitates, lowering the hydrophobicity of the membrane and degrading the Cassie-Baxter state into the Wenzel state. In the Wenzel state the precipitates are more likely to settle onto or crystallize on the membrane and an increase in the rate of water flux decline is observed. In contrast, the much higher mass of calcium precipitating in the BAC treated ROC likely deteriorates the Cassie-Baxter state more rapidly than the slower precipitation rates observed in the softened ROC.

Preserving or enhancing the Cassie-Baxter state in MD may be an effective way to mitigate fouling and scaling and methods can be categorized as either membrane cleaning or membrane materials. An ideal membrane cleaning method would restore both the water flux and the Cassie-Baxter state. Notably, Rezaei et. al. developed a method to recharge the air layer on hydrophobic membranes to prevent wetting by surfactants [63] which may be an effective cleaning method that meets these criteria. Novel membrane materials have been shown to protect the membrane from scaling by supersaturated NaCl solutions [41, 62] and gypsum solutions [64] for longer than their unmodified counterparts. Other modified membranes have been developed to address fouling by oil or other hydrophobic organic matter [65]. Although these membranes show great promise for addressing scaling in MD they are typically modified commercial membranes [66] that are currently unavailable at scale due in part to the use of harsh chemicals such as perflourinated compounds required and complex synthesis processes [67]. Therefore, employing pretreatment strategies that selectively remove the scalants or foulants of concerns along with periodic membrane cleanings may be an area for future research to mitigate membrane scaling and fouling and preserving the Cassie-Baxter state in MD. Alternative strategies to reduce membrane scaling could also include antiscalants or operating at lower feed temperatures to minimize calcium precipitation. However, tradeoffs arise when operating at lower temperatures as water production rates and energy efficiency decrease at lower operating temperatures [6].

4. Conclusion

Membrane distillation can be an effective technology that can simultaneously recover and concentrate water reuse ROC achieving near zero liquid discharge. This study identified relevant foulants, scalants, and potential mitigation strategies when using water reuse ROC as the feed solution for MD. Calcium salts were the dominant scalants, and removing calcium with FBCR-ion exchange was an effective pretreatment strategy to minimize the decline in water flux. Despite the presence of natural organic matter in the feed solution, minimal organic fouling was observed likely because the organics were hydrophilic, thus eliminating hydrophobic-hydrophobic interactions with the membrane. An untargeted HPLC method was developed to determine the hydrophobicity of organic matter in complex solutions. This method is a novel application of reverse phase HPLC analysis and may be particularly useful in rapidly assessing the potential for membrane fouling via hydrophobic-hydrophobic interactions and selecting cleaning and pre-treatment strategies; thus, prolonging membrane lifetime and reducing

operational costs. Finally, it was observed that the rate of scaling increases as the membrane becomes less hydrophobic. Therefore, in addition to selecting hydrophobic membranes, selective pretreatment strategies and membrane cleaning can preserve the Cassie-Baxter state of the MD membrane and inhibit membrane wetting.

Acknowledgments

U.S. Bureau of Reclamation, agreement no. R18AC00115, Phoenix Water (Sponsor Award No. 147778-0/147778-PSA-003), and the U.S. Department of Energy RAPID Program (Project #8.10) funded this work. The authors also acknowledge Clarcor for donating the bench-scale MD membranes.

5. References

[1] X. Zhang, Y. Liu, Reverse osmosis concentrate: An essential link for closing loop of municipal wastewater reclamation towards urban sustainability, Chemical Engineering Journal, 421 (2021) 127773.
[2] E.W. Tow, A.L. Hartman, A. Jaworowski, I. Zucker, S. Kum, M. AzadiAghdam, E.R. Blatchley III, A. Achilli, H. Gu, G.M. Urper, Modeling the energy consumption of potable water reuse schemes, Water research X, 13 (2021) 100126.
[3] D.M. Warsinger, S. Chakraborty, E.W. Tow, M.H. Plumlee, C. Bellona, S. Loutatidou, L. Karimi, A.M. Mikelonis, A. Achilli, A. Ghassemi, L.P. Padhye, S.A. Snyder, S. Curcio, C.D. Vecitis, H.A. Arafat, J.H. Lienhard, A review of polymeric membranes and processes for potable water reuse, Progress in Polymer Science, 81 (2018) 209-237.
[4] T. Tong, M. Elimelech, The Global Rise of Zero Liquid Discharge for Wastewater Management: Drivers, Technologies, and Future Directions, Environ. Sci. Technol., 50 (2016) 6846-6855.
[5] M. Hardikar, L.A. Ikner, V. Felix, L.K. Presson, A.B. Rabe, K.L. Hickenbottom, A. Achilli, Membrane distillation provides a dual barrier for coronavirus and bacteriophage removal, Environmental Science & Technology Letters, 8 (2021) 713-718.
[6] M. Hardikar, I. Marquez, T. Phakdon, A.E. Sáez, A. Achilli, Scale-up of membrane distillation systems using bench-scale data, Desalination, 530 (2022) 115654.
[7] M. Hardikar, I. Marquez, A. Achilli, Emerging investigator series: membrane distillation and high salinity: analysis and implications, Environmental Science: Water Research & Technology, 6 (2020) 1538-1552.
[8] V. Karanikola, C. Boo, J. Rolf, M. Elimelech, Engineered Slippery Surface to Mitigate Gypsum Scaling in Membrane Distillation for Treatment of Hypersaline Industrial Wastewaters, Environ. Sci. Technol., 52 (2018) 14362-14370.
[9] F. Li, J. Huang, Q. Xia, M. Lou, B. Yang, Q. Tian, Y. Liu, Direct contact membrane distillation for the treatment of industrial dyeing wastewater and characteristic pollutants, Separation and Purification Technology, 195 (2018) 83-91.

[10] C. Boo, J. Lee, M. Elimelech, Omniphobic Polyvinylidene Fluoride (PVDF) Membrane for Desalination of Shale Gas Produced Water by Membrane Distillation, Environ. Sci. Technol., 50 (2016) 12275-12282.
[11] X. Du, Z. Zhang, K.H. Carlson, J. Lee, T. Tong, Membrane fouling and reusability in membrane distillation of shale oil and gas produced water: Effects of membrane surface wettability, Journal of Membrane Science, 567 (2018) 199-208.
[12] L. Zou, P. Gusnawan, G. Zhang, J. Yu, Novel Janus composite hollow fiber membrane-based direct contact membrane distillation (DCMD) process for produced water desalination, Journal of Membrane Science, 597 (2020) 117756.
[13] C.R. Martinetti, A.E. Childress, T.Y. Cath, High recovery of concentrated RO brines using forward osmosis and membrane distillation, Journal of Membrane Science, 331 (2009) 31-39.
[14] J.-P. Mericq, S. Laborie, C. Cabassud, Vacuum membrane distillation of seawater reverse osmosis brines, Water Research, 44 (2010) 5260-5273.
[15] G. Naidu, S. Jeong, Y. Choi, S. Vigneswaran, Membrane distillation for wastewater reverse osmosis concentrate treatment with water reuse potential, Journal of Membrane Science, 524 (2017) 565-575.
[16] M.T.T. Ngo, B.Q. Diep, H. Sano, Y. Nishimura, S. Boivin, H. Kodamatani, H. Takeuchi, S.C.W. Sakti, T. Fujioka, Membrane distillation for achieving high water recovery for potable water reuse, Chemosphere, 288 (2022) 132610.
[17] O.R. Lokare, P. Ji, S. Wadekar, G. Dutt, R.D. Vidic, Concentration polarization in membrane distillation: I. Development of a laser-based spectrophotometric method for in-situ characterization, Journal of Membrane Science, 581 (2019) 462-471.
[18] A.B.D. Cassie, S. Baxter, Wettability of porous surfaces, Transactions of the Faraday society, 40 (1944) 546-551.
[19] T. Horseman, C. Su, K.S.S. Christie, S. Lin, Highly Effective Scaling Mitigation in Membrane Distillation Using a Superhydrophobic Membrane with Gas Purging, Environmental Science & Technology Letters, 6 (2019) 423-429.
[20] N.A. Patankar, Thermodynamics of Trapping Gases for Underwater Superhydrophobicity, Langmuir, 32 (2016) 7023-7028.
[21] C. Su, T. Horseman, H. Cao, K. Christie, Y. Li, S. Lin, Robust Superhydrophobic Membrane for Membrane Distillation with Excellent Scaling Resistance, Environ. Sci. Technol., 53 (2019) 11801-11809.
[22] R.N. Wenzel, Resistance of Solid Surfaces to Wetting by Water, Industrial & Engineering Chemistry, 28 (1936) 988-994.
[23] S. Lin, S. Nejati, C. Boo, Y. Hu, C.O. Osuji, M. Elimelech, Omniphobic Membrane for Robust Membrane Distillation, Environmental Science & Technology Letters, 1 (2014) 443-447.
[24] K.J. Lu, Y. Chen, T.-S. Chung, Design of omniphobic interfaces for membrane distillation – A review, Water Research, 162 (2019) 64-77.
[25] S. Jeong, K.G. Song, J. Kim, J. Shin, S.K. Maeng, J. Park, Feasibility of membrane distillation process for potable water reuse: A barrier for dissolved organic matters and pharmaceuticals, Journal of Hazardous Materials, 409 (2021) 124499.
[26] H.-C. Kim, J. Shin, S. Won, J.-Y. Lee, S.K. Maeng, K.G. Song, Membrane distillation combined with an anaerobic moving bed biofilm reactor for treating municipal wastewater, Water Research, 71 (2015) 97-106.

[27] K. Rajwade, A.C. Barrios, S. Garcia-Segura, F. Perreault, Pore wetting in membrane distillation treatment of municipal wastewater desalination brine and its mitigation by foam fractionation, Chemosphere, 257 (2020) 127214.
[28] A.L. McGaughey, A.E. Childress, Wetting indicators, modes, and trade-offs in membrane distillation, Journal of Membrane Science, 642 (2022) 119947.
[29] T. Horseman, Y. Yin, K.S.S. Christie, Z. Wang, T. Tong, S. Lin, Wetting, Scaling, and Fouling in Membrane Distillation: State-of-the-Art Insights on Fundamental Mechanisms and Mitigation Strategies, ACS EST Eng., (2020).
[30] C. Boo, S. Hong, M. Elimelech, Relating Organic Fouling in Membrane Distillation to Intermolecular Adhesion Forces and Interfacial Surface Energies, Environ. Sci. Technol., 52 (2018) 14198-14207.
[31] S.A. Huber, A. Balz, M. Abert, W. Pronk, Characterisation of aquatic humic and non-humic matter with size-exclusion chromatography – organic carbon detection – organic nitrogen detection (LC-OCD-OND), Water Research, 45 (2011) 879-885.
[32] J.A. Leenheer, J.-P. Croue, Peer Reviewed: Characterizing Aquatic Dissolved Organic Matter, Environ. Sci. Technol., 37 (2003) 18A-26A.
[33] W.-T. Li, S.-Y. Chen, Z.-X. Xu, Y. Li, C.-D. Shuang, A.-M. Li, Characterization of Dissolved Organic Matter in Municipal Wastewater Using Fluorescence PARAFAC Analysis and Chromatography Multi-Excitation/Emission Scan: A Comparative Study, Environ. Sci. Technol., 48 (2014) 2603-2609.
[34] W.-T. Li, Z.-X. Xu, A.-M. Li, W. Wu, Q. Zhou, J.-N. Wang, HPLC/HPSEC-FLD with multi-excitation/emission scan for EEM interpretation and dissolved organic matter analysis, Water Research, 47 (2013) 1246-1256.
[35] K. Xiao, Y. Shen, S. Liang, J. Tan, X. Wang, P. Liang, X. Huang, Characteristic Regions of the Fluorescence Excitation–Emission Matrix (EEM) To Identify Hydrophobic/Hydrophilic Contents of Organic Matter in Membrane Bioreactors, Environ. Sci. Technol., 52 (2018) 11251-11258.
[36] J. Rolf, T. Cao, X. Huang, C. Boo, Q. Li, M. Elimelech, Inorganic Scaling in Membrane Desalination: Models, Mechanisms, and Characterization Methods, Environ. Sci. Technol., 56 (2022) 7484-7511.
[37] K.S.S. Christie, Y. Yin, S. Lin, T. Tong, Distinct Behaviors between Gypsum and Silica Scaling in Membrane Distillation, Environ. Sci. Technol., 54 (2020) 568-576.
[38] S. Srisurichan, R. Jiraratananon, Humic acid fouling in the membrane distillation process, Desalination, 174 (2005) 63-72.
[39] Z. Zhang, X. Du, K.H. Carlson, C.A. Robbins, T. Tong, Effective treatment of shale oil and gas produced water by membrane distillation coupled with precipitative softening and walnut shell filtration, Desalination, 454 (2019) 82-90.
[40] J.A. Bush, J. Vanneste, E.M. Gustafson, C.A. Waechter, D. Jassby, C.S. Turchi, T.Y. Cath, Prevention and management of silica scaling in membrane distillation using pH adjustment, Journal of Membrane Science, 554 (2018) 366-377.
[41] Z. Xiao, R. Zheng, Y. Liu, H. He, X. Yuan, Y. Ji, D. Li, H. Yin, Y. Zhang, X.-M. Li, T. He, Slippery for scaling resistance in membrane distillation: A novel porous micropillared superhydrophobic surface, Water Research, 155 (2019) 152-161.
[42] K.L. Hickenbottom, T.Y. Cath, Sustainable operation of membrane distillation for enhancement of mineral recovery from hypersaline solutions, Journal of Membrane Science, 454 (2014) 426-435.

[43] B. Messnaoui, T. Bounahmidi, On the modeling of calcium sulfate solubility in aqueous solutions, Fluid Phase Equilibria, 244 (2006) 117-127.
[44] D.M. Warsinger, J. Swaminathan, H.W. Chung, S. Jeong, J.H. Lienhard V, Effect of Filtration and Particulate Fouling in Membrane Distillation, in: International Desalination Association World Congress on Desalination and Water Reuse, International Desalination Association, San Diego, CA, USA, 2015.
[45] F. He, K.K. Sirkar, J. Gilron, Effects of antiscalants to mitigate membrane scaling by direct contact membrane distillation, Journal of Membrane Science, 345 (2009) 53-58.
[46] P. Zhang, P. Knötig, S. Gray, M. Duke, Scale reduction and cleaning techniques during direct contact membrane distillation of seawater reverse osmosis brine, Desalination, 374 (2015) 20-30.
[47] F. Qu, Z. Yan, H. Yu, G. Fan, H. Pang, H. Rong, J. He, Effect of residual commercial antiscalants on gypsum scaling and membrane wetting during direct contact membrane distillation, Desalination, 486 (2020) 114493.
[48] Y. Chen, J.R. Davis, C.H. Nguyen, J.C. Baygents, J. Farrell, Electrochemical Ion-Exchange Regeneration and Fluidized Bed Crystallization for Zero-Liquid-Discharge Water Softening, Environ. Sci. Technol., 50 (2016) 5900-5907.
[49] M. AzadiAghdam, M. Park, I.J. Lopez-Prieto, A. Achilli, S.A. Snyder, J. Farrell, Pretreatment for water reuse using fluidized bed crystallization, Journal of Water Process Engineering, 35 (2020) 101226.
[50] K.L. Hickenbottom, T.Y. Cath, Methods for Sustainable Membrane Distillation Concentration of Hypersaline Streams, US 20130327711, June 11, 2013.
[51] C. Hansch, A. Leo, D. Hoekman, Exploring QSAR: Hydrophobic, electronic, and steric constants, in: C. Hansch, A. Leo, D.H. Hoekman (Eds.) ACS Professional Reference Book, American Chemical Society, Washington, DC, 1995.
[52] J.A. Bush, J. Vanneste, T.Y. Cath, Membrane distillation for concentration of hypersaline brines from the Great Salt Lake: Effects of scaling and fouling on performance, efficiency, and salt rejection, Separation and Purification Technology, 170 (2016) 78-91.
[53] R. Zhu, L. Zacharias, K.M. Wooding, W. Peng, Y. Mechref, Chapter Twenty-One - Glycoprotein Enrichment Analytical Techniques: Advantages and Disadvantages, in: A.K. Shukla (Ed.) Methods in Enzymology, Academic Press, 2017, pp. 397-429.
[54] P. Žuvela, M. Skoczylas, J. Jay Liu, T. Bączek, R. Kaliszan, M.W. Wong, B. Buszewski, Column Characterization and Selection Systems in Reversed-Phase High-Performance Liquid Chromatography, Chemical Reviews, 119 (2019) 3674-3729.
[55] Z. El Rassi, Chapter 2 - Reversed-phase and hydrophobic interaction chromatography of carbohydrates and glycoconjugates, in: Z. El Rassi (Ed.) Carbohydrate Analysis by Modern Liquid Phase Separation Techniques (Second Edition), Elsevier, Amsterdam, 2021, pp. 35-124.
[56] S.C. Moldoveanu, V. David, Chapter 5 - Retention Mechanisms in Different HPLC Types, in: S.C. Moldoveanu, V. David (Eds.) Essentials in Modern HPLC Separations, Elsevier, 2013, pp. 145-190.
[57] K.-G. Lu, M. Li, H. Huang, Silica scaling of reverse osmosis membranes preconditioned by natural organic matter, Science of The Total Environment, 746 (2020) 141178.
[58] A.N. Quay, T. Tong, S.M. Hashmi, Y. Zhou, S. Zhao, M. Elimelech, Combined Organic Fouling and Inorganic Scaling in Reverse Osmosis: Role of Protein–Silica Interactions, Environ. Sci. Technol., 52 (2018) 9145-9153.

[59] J. Fernández-Sempere, F. Ruiz-Beviá, P. García-Algado, R. Salcedo-Díaz, Experimental study of concentration polarization in a crossflow reverse osmosis system using Digital Holographic Interferometry, Desalination, 257 (2010) 36-45.
[60] S.O. Olatunji, L.M. Camacho, Heat and Mass Transport in Modeling Membrane Distillation Configurations: A Review, Frontiers in Energy Research, 6 (2018).
[61] M. Shakaib, S.M.F. Hasani, I. Ahmed, R.M. Yunus, A CFD study on the effect of spacer orientation on temperature polarization in membrane distillation modules, Desalination, 284 (2012) 332-340.
[62] A.L. McGaughey, P. Karandikar, M. Gupta, A.E. Childress, Hydrophobicity versus Pore Size: Polymer Coatings to Improve Membrane Wetting Resistance for Membrane Distillation, ACS Applied Polymer Materials, 2 (2020) 1256-1267.
[63] M. Rezaei, D.M. Warsinger, J.H. Lienhard V, W.M. Samhaber, Wetting prevention in membrane distillation through superhydrophobicity and recharging an air layer on the membrane surface, Journal of Membrane Science, 530 (2017) 42-52.
[64] Y. Chen, K.J. Lu, T.-S. Chung, An omniphobic slippery membrane with simultaneous anti-wetting and anti-scaling properties for robust membrane distillation, Journal of Membrane Science, 595 (2020) 117572.
[65] K. Wang, D. Hou, J. Wang, Z. Wang, B. Tian, P. Liang, Hydrophilic surface coating on hydrophobic PTFE membrane for robust anti-oil-fouling membrane distillation, Applied Surface Science, 450 (2018) 57-65.
[66] M. Qasim, I.U. Samad, N.A. Darwish, N. Hilal, Comprehensive review of membrane design and synthesis for membrane distillation, Desalination, 518 (2021) 115168.
[67] Y. Liao, G. Zheng, J.J. Huang, M. Tian, R. Wang, Development of robust and superhydrophobic membranes to mitigate membrane scaling and fouling in membrane distillation, Journal of Membrane Science, 601 (2020) 117962.

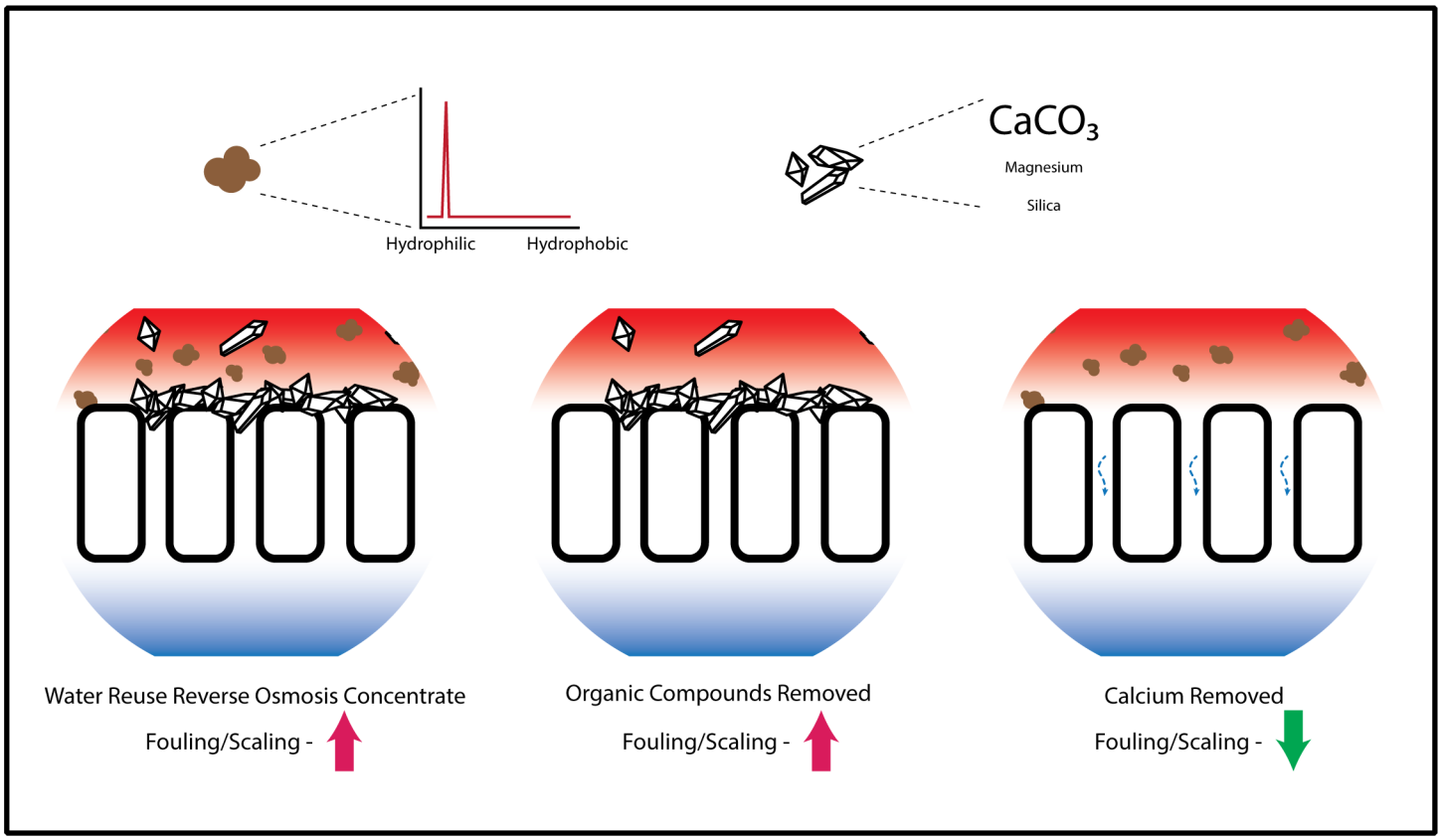
Hydrophilic
Hydrophobic
$CaCO_3$
Magnesium
Silica
Water Reuse Reverse Osmosis Concentrate
Fouling/Scaling -
Organic Compounds Removed
Fouling/Scaling -
Calcium Removed
Fouling/Scaling -